Frequency comb offset detection using supercontinuum generation in silicon nitride waveguides

A. S. Mayer,[1,*] A. Klenner,[1] A. R. Johnson,[2] K. Luke,[3] M. R. E. Lamont,[2,3,4] Y. Okawachi,[2] M. Lipson,[3,4] A. L. Gaeta,[2,4] and U. Keller[1]

[1]*Department of Physics, Institute of Quantum Electronics, ETH Zurich, 8093 Zurich, Switzerland*
[2]*School of Applied and Engineering Physics, Cornell University, Ithaca, New York 14853, USA*
[3]*School of Electrical and Computer Engineering, Cornell University, Ithaca, New York 14853, USA*
[4]*Kavli Institute at Cornell for Nanoscale Science, Cornell University, Ithaca, New York 14853, USA*
[*]*mayeral@phys.ethz.ch*

Abstract: We present the first direct carrier-envelope-offset (CEO) frequency detection of a modelocked laser based on supercontinuum generation (SCG) in a CMOS-compatible silicon nitride (Si_3N_4) waveguide. With a coherent supercontinuum spanning more than 1.5 octaves from visible to beyond telecommunication wavelengths, we achieve self-referencing of SESAM modelocked diode-pumped Yb:CALGO lasers using standard *f*-to-2*f* interferometry. We directly obtain without amplification strong CEO beat signals for both a 100-MHz and 1-GHz pulse repetition rate laser. High signal-to-noise ratios (SNR) of > 25 dB and even > 30 dB have been generated with only 30 pJ and 36 pJ of coupled pulse energy from the megahertz and gigahertz laser respectively. We compare these results to self-referencing using a commercial photonic crystal fiber and find that the required peak power for CEO beat detection with a comparable SNR is lowered by more than an order of magnitude when using a Si_3N_4 waveguide.

OCIS codes: (320.7090) Ultrafast lasers; (320.6629) Supercontinuum generation; (230.7370) Waveguides; (130.4310) Nonlinear; (190.4390) Nonlinear optics, integrated optics.

References and links

1. H. R. Telle, G. Steinmeyer, A. E. Dunlop, J. Stenger, D. H. Sutter, and U. Keller, "Carrier-envelope offset phase control: A novel concept for absolute optical frequency measurement and ultrashort pulse generation," Appl. Phys. B **69**(4), 327–332 (1999).
2. D. J. Jones, S. A. Diddams, J. K. Ranka, A. Stentz, R. S. Windeler, J. L. Hall, and S. T. Cundiff, "Carrier-envelope phase control of femtosecond mode-locked lasers and direct optical frequency synthesis," Science **288**(5466), 635–639 (2000).
3. A. Apolonski, A. Poppe, G. Tempea, C. Spielmann, T. Udem, R. Holzwarth, T. W. Hänsch, and F. Krausz, "Controlling the phase evolution of few-cycle light pulses," Phys. Rev. Lett. **85**(4), 740–743 (2000).
4. U. Keller, "Ultrafast solid-state laser oscillators: a success story for the last 20 years with no end in sight," Appl. Phys. B **100**(1), 15–28 (2010).
5. S. R. Leone, C. W. McCurdy, J. Burgdorfer, L. S. Cederbaum, Z. Chang, N. Dudovich, J. Feist, C. H. Greene, M. Ivanov, R. Kienberger, U. Keller, M. F. Kling, Z.-H. Loh, T. Pfeifer, A. N. Pfeiffer, R. Santra, K. Schafer, A. Stolow, U. Thumm, and M. J. J. Vrakking, "What will it take to observe processes in 'real time'?" Nat. Photonics **8**(3), 162–166 (2014).
6. B. A. Wilt, L. D. Burns, E. T. Wei Ho, K. K. Ghosh, E. A. Mukamel, and M. J. Schnitzer, "Advances in light microscopy for neuroscience," Annu. Rev. Neurosci. **32**(1), 435–506 (2009).
7. I. Hartl, X. D. Li, C. Chudoba, R. K. Ghanta, T. H. Ko, J. G. Fujimoto, J. K. Ranka, and R. S. Windeler, "Ultrahigh-resolution optical coherence tomography using continuum generation in an air-silica microstructure optical fiber," Opt. Lett. **26**(9), 608–610 (2001).
8. R. Holzwarth, T. Udem, T. W. Hänsch, J. C. Knight, W. J. Wadsworth, and P. S. J. Russell, "Optical frequency synthesizer for precision spectroscopy," Phys. Rev. Lett. **85**(11), 2264–2267 (2000).

#238286 - $15.00 USD Received 17 Apr 2015; revised 21 May 2015; accepted 24 May 2015; published 3 Jun 2015

9. H. S. Margolis, "Spectroscopic applications of femtosecond optical frequency combs," Chem. Soc. Rev. **41**(15), 5174–5184 (2012).
10. M. T. Murphy, T. Udem, R. Holzwarth, A. Sizmann, L. Pasquini, C. Araujo-Hauk, H. Dekker, S. D'Odorico, M. Fischer, T. W. Hänsch, and A. Manescau, "High-precision wavelength calibration of astronomical spectrographs with laser frequency combs," Mon. Not. R. Astron. Soc. **380**(2), 839–847 (2007).
11. S. A. Diddams, J. C. Bergquist, S. R. Jefferts, and C. W. Oates, "Standards of time and frequency at the outset of the 21st century," Science **306**(5700), 1318–1324 (2004).
12. J. Millo, R. Boudot, M. Lours, P. Y. Bourgeois, A. N. Luiten, Y. Le Coq, Y. Kersalé, and G. Santarelli, "Ultra-low-noise microwave extraction from fiber-based optical frequency comb," Opt. Lett. **34**(23), 3707–3709 (2009).
13. A. Bartels, D. Heinecke, and S. A. Diddams, "10-GHz self-referenced optical frequency comb," Science **326**(5953), 681 (2009).
14. D. E. Spence, P. N. Kean, and W. Sibbett, "60-fsec pulse generation from a self-mode-locked Ti:sapphire laser," Opt. Lett. **16**(1), 42–44 (1991).
15. G. Steinmeyer, D. H. Sutter, L. Gallmann, N. Matuschek, and U. Keller, "Frontiers in ultrashort pulse generation: pushing the limits in linear and nonlinear optics," Science **286**(5444), 1507–1512 (1999).
16. S. Schilt, V. Dolgovskiy, N. Bucalovic, C. Schori, M. C. Stumpf, G. Domenico, S. Pekarek, A. E. H. Oehler, T. Südmeyer, U. Keller, and P. Thomann, "Noise properties of an optical frequency comb from a SESAM-mode-locked 1.5-μm solid-state laser stabilized to the 10^{-13} level," Appl. Phys. B **109**(3), 1–12 (2012).
17. A. Schlatter, B. Rudin, S. C. Zeller, R. Paschotta, G. J. Spühler, L. Krainer, N. Haverkamp, H. R. Telle, and U. Keller, "Nearly quantum-noise-limited timing jitter from miniature Er:Yb:glass lasers," Opt. Lett. **30**(12), 1536–1538 (2005).
18. R. Paschotta, A. Schlatter, S. C. Zeller, H. R. Telle, and U. Keller, "Optical phase noise and carrier-envelope offset noise of mode-locked lasers," Appl. Phys. B **82**(2), 265–273 (2006).
19. U. Keller, K. J. Weingarten, F. X. Kärtner, D. Kopf, B. Braun, I. D. Jung, R. Fluck, C. Hönninger, N. Matuschek, and J. Aus der Au, "Semiconductor saturable absorber mirrors (SESAMs) for femtosecond to nanosecond pulse generation in solid-state lasers," IEEE J. Sel. Top. Quantum Electron. **2**(3), 435–453 (1996).
20. A. Klenner, S. Schilt, T. Südmeyer, and U. Keller, "Gigahertz frequency comb from a diode-pumped solid-state laser," Opt. Express **22**(25), 31008–31019 (2014).
21. C. A. Zaugg, A. Klenner, M. Mangold, A. S. Mayer, S. M. Link, F. Emaury, M. Golling, E. Gini, C. J. Saraceno, B. W. Tilma, and U. Keller, "Gigahertz self-referenceable frequency comb from a semiconductor disk laser," Opt. Express **22**(13), 16445–16455 (2014).
22. C. R. Phillips, C. Langrock, J. S. Pelc, M. M. Fejer, I. Hartl, and M. E. Fermann, "Supercontinuum generation in quasi-phasematched waveguides," Opt. Express **19**(20), 18754–18773 (2011).
23. C. R. Phillips, C. Langrock, J. S. Pelc, M. M. Fejer, J. Jiang, M. E. Fermann, and I. Hartl, "Supercontinuum generation in quasi-phase-matched $LiNbO_3$ waveguide pumped by a Tm-doped fiber laser system," Opt. Lett. **36**(19), 3912–3914 (2011).
24. C. Langrock, M. M. Fejer, I. Hartl, and M. E. Fermann, "Generation of octave-spanning spectra inside reverse-photon-exchanged periodically poled lithium niobate waveguides," Opt. Lett. **32**(17), 2478–2480 (2007).
25. I. Hartl, G. Imeshev, M. Fermann, C. Langrock, and M. Fejer, "Integrated self-referenced frequency-comb laser based on a combination of fiber and waveguide technology," Opt. Express **13**(17), 6490–6496 (2005).
26. M. R. Lamont, B. Luther-Davies, D.-Y. Choi, S. Madden, and B. J. Eggleton, "Supercontinuum generation in dispersion engineered highly nonlinear (γ = 10 /W/m) As_2S_3) chalcogenide planar waveguide," Opt. Express **16**(19), 14938–14944 (2008).
27. N. D. Psaila, R. R. Thomson, H. T. Bookey, S. Shen, N. Chiodo, R. Osellame, G. Cerullo, A. Jha, and A. K. Kar, "Supercontinuum generation in an ultrafast laser inscribed chalcogenide glass waveguide," Opt. Express **15**(24), 15776–15781 (2007).
28. K. F. Lee, N. Granzow, M. A. Schmidt, W. Chang, L. Wang, Q. Coulombier, J. Troles, N. Leindecker, K. L. Vodopyanov, P. G. Schunemann, M. E. Fermann, P. S. J. Russell, and I. Hartl, "Midinfrared frequency combs from coherent supercontinuum in chalcogenide and optical parametric oscillation," Opt. Lett. **39**(7), 2056–2059 (2014).
29. F. Leo, S.-P. Gorza, S. Coen, B. Kuyken, and G. Roelkens, "Coherent supercontinuum generation in a silicon photonic wire in the telecommunication wavelength range," Opt. Lett. **40**(1), 123–126 (2015).
30. R. K. W. Lau, M. R. E. Lamont, A. G. Griffith, Y. Okawachi, M. Lipson, and A. L. Gaeta, "Octave-spanning mid-infrared supercontinuum generation in silicon nanowaveguides," Opt. Lett. **39**(15), 4518–4521 (2014).
31. J. Safioui, F. Leo, B. Kuyken, S.-P. Gorza, S. K. Selvaraja, R. Baets, P. Emplit, G. Roelkens, and S. Massar, "Supercontinuum generation in hydrogenated amorphous silicon waveguides at telecommunication wavelengths," Opt. Express **22**(3), 3089–3097 (2014).
32. D. Duchesne, M. Peccianti, M. R. E. Lamont, M. Ferrera, L. Razzari, F. Légaré, R. Morandotti, S. Chu, B. E. Little, and D. J. Moss, "Supercontinuum generation in a high index doped silica glass spiral waveguide," Opt. Express **18**(2), 923–930 (2010).
33. J. M. Chavez Boggio, D. Bodenmüller, T. Fremberg, R. Haynes, M. M. Roth, R. Eisermann, M. Lisker, L. Zimmermann, and M. Böhm, "Dispersion engineered silicon nitride waveguides by geometrical and refractive-index optimization," J. Opt. Soc. Am. B **31**(11), 2846–2857 (2014).
34. R. Halir, Y. Okawachi, J. S. Levy, M. A. Foster, M. Lipson, and A. L. Gaeta, "Ultrabroadband supercontinuum generation in a CMOS-compatible platform," Opt. Lett. **37**(10), 1685–1687 (2012).

#238286 - $15.00 USD Received 17 Apr 2015; revised 21 May 2015; accepted 24 May 2015; published 3 Jun 2015

35. B. Kuyken, T. Ideguchi, S. Holzner, M. Yan, T. W. Hänsch, J. Van Campenhout, P. Verheyen, S. Coen, F. Leo, R. Baets, G. Roelkens, and N. Picqué, "An octave-spanning mid-infrared frequency comb generated in a silicon nanophotonic wire waveguide," Nat. Commun. **6**, 6310 (2015).
36. Y. Okawachi, K. Saha, J. S. Levy, Y. H. Wen, M. Lipson, and A. L. Gaeta, "Octave-spanning frequency comb generation in a silicon nitride chip," Opt. Lett. **36**(17), 3398–3400 (2011).
37. D. J. Moss, R. Morandotti, A. L. Gaeta, and M. Lipson, "New CMOS-compatible platforms based on silicon nitride and Hydex for nonlinear optics," Nat. Photonics **7**(8), 597–607 (2013).
38. K. Ikeda, R. E. Saperstein, N. Alic, and Y. Fainman, "Thermal and Kerr nonlinear properties of plasma-deposited silicon nitride/ silicon dioxide waveguides," Opt. Express **16**(17), 12987–12994 (2008).
39. B. W. Tilma, M. Mangold, C. A. Zaugg, S. M. Link, D. Waldburger, A. Klenner, A. S. Mayer, E. Gini, M. Golling, and U. Keller, "Recent advances in ultrafast semiconductor disk lasers" Light: Science and Applications (to be published).
40. J. Cardenas, C. B. Poitras, K. Luke, L. Lian-Wee, P. A. Morton, and M. Lipson, "High coupling efficiency etched facet tapers in silicon waveguides," IEEE Photon. Technol. Lett. **26**(23), 2380–2382 (2014).
41. J. S. Levy, M. A. Foster, A. L. Gaeta, and M. Lipson, "Harmonic generation in silicon nitride ring resonators," Opt. Express **19**(12), 11415–11421 (2011).
42. J. Andreasen, A. Bahl, and M. Kolesik, "Spatial effects in supercontinuum generation in waveguides," Opt. Express **22**(21), 25756–25767 (2014).
43. M. Kuznetsov, F. Hakimi, R. Sprague, and A. Mooradian, "High-power (>0.5-W CW) diode-pumped vertical-external-cavity surface-emitting semiconductor lasers with circular TEM00 beams," IEEE Photon. Technol. Lett. **9**(8), 1063–1065 (1997).
44. U. Keller and A. C. Tropper, "Passively modelocked surface-emitting semiconductor lasers," Phys. Rep. **429**(2), 67–120 (2006).
45. D. J. H. C. Maas, A.-R. Bellancourt, B. Rudin, M. Golling, H. J. Unold, T. Südmeyer, and U. Keller, "Vertical integration of ultrafast semiconductor lasers," Appl. Phys. B **88**(4), 493–497 (2007).

1. Introduction

Stabilized frequency combs based on ultrafast lasers [1–4] have been a significant breakthrough with many important applications in various fields within chemistry, biology and physics. The frequency comb offset (i.e. the carrier envelope offset, CEO) is directly related to the exact position of the electric field underneath the pulse envelope [1] which has become important for highly nonlinear systems and attosecond science [5]. The broad coherent optical spectra obtained by supercontinuum generation (SCG) are the basis for many biomedical imaging techniques [6, 7]. Stabilized optical frequency combs enable the measurement of optical frequencies with a very high precision, which is essential for many spectroscopic applications ranging from the detection of molecular transitions to the calibration of astronomical spectrographs [8–10]. In the context of optical frequency metrology, frequency combs provide a direct link between optical and microwave frequencies, a property that has been exploited to strongly reduce the complexity of the optical atomic clocks, leading to a new generation of systems for the primary definition of time [11]. Currently, the comb line spacing obtained from commercially available sources is usually not exceeding a few hundred megahertz. Gigahertz line spacings and an increased power per mode would however be beneficial for important applications such as the generation of ultra-low noise microwave signals [12] or to enable the resolution of individual lines in calibration procedures for astronomical spectrographs [10].

Great efforts have been made to obtain a stabilized 10-GHz frequency comb from a Ti:sapphire laser [13]. However, Ti:sapphire systems still rely on an expensive and complex single-mode pumping scheme and Kerr lens modelocking [14] requires operation at the edge of the cavity stability range [15]. The cost-efficient and more compact fiber-based frequency comb sources on the other hand work in a regime with comparably high cavity losses, which reduces the cavity quality factor (Q) and results in deteriorated noise properties [16–18]. The limited power of gigahertz fiber laser oscillators has not allowed for comb stabilization without additional amplification.

Low noise properties and reliable operation can be obtained using diode-pumped solid-state lasers (DPSSL's) modelocked with a semiconductor saturable absorber mirror (SESAM) [19]. Recently, the successful stabilization of the frequency comb offset from a gigahertz SESAM-modelocked DPSSL has been demonstrated [20]. The short pulses (64 fs) combined

#238286 - $15.00 USD Received 17 Apr 2015; revised 21 May 2015; accepted 24 May 2015; published 3 Jun 2015

with an average output power of more than 1 W provides sufficient peak power for coherent octave-spanning SCG in a photonic crystal fiber (PCF) and CEO frequency (f_{CEO}) detection using self-referencing in an *f*-to-2*f* interferometer without the need for external amplification or compression of the pulses. Furthermore, the first detection of the comb offset frequency from a SESAM modelocked semiconductor laser has become possible [21], however, at this point additional external amplification and compression was required.

The key requirement to perform self-referencing frequency comb offset detection is a modelocked spectrum and depending on the modelocked bandwidth different techniques have been proposed using one or two nonlinear processes [1]. The simplest detection with only one nonlinear process (i.e. referred to as the *f*-to-2*f* technique today) requires a coherent octave-spanning SC which is typically obtained by additionally broadening the pulse spectrum in an external nonlinear device. To date silica-based optical fibers have been the most common SCG platform to self-reference modelocked lasers. The most efficient spectral broadening is generally obtained if soliton effects dominate the SCG process, i.e. if the fiber is pumped within its anomalous group velocity dispersion (GVD). Standard silica fibers provide anomalous GVD for wavelengths above ≈1.3 μm. For lasers operating in the 1-μm regime however, the design of fibers with anomalous GVD for the pump wavelength is more complex, involving for instance a microstructured cross-section. Only a limited choice of such fibers is commercially available and the required peak power remains a challenge particularly for lasers at high repetition rate and/or with pulse durations longer than 100 fs.

Recent investigations have focused on reducing the requirements for coherent SCG by using novel nonlinear devices. The research on chip-based supercontinuum generation in materials such as periodically poled lithium niobate (PPLN) [22–25], chalcogenide [26–28], silicon [29, 30], amorphous silicon [31], Hydex [32] and silicon nitride (Si_3N_4) [33, 34] has opened up interesting new possibilities in terms of compactness, nonlinearity and dispersion engineering. Chip-based self-referencing of modelocked lasers has so far only been demonstrated with PPLN waveguides using pulse energies of 600 pJ from an erbium-doped fiber laser [25], and 7 nJ from of a thulium-doped fiber laser system [23].

Silicon waveguides have the advantage to provide very high nonlinearities and thus reduce the pulse energy requirements. SCG is however only possible with pump wavelengths longer than ≈1.1 μm (absorption edge). Furthermore, silicon-based devices allow for low-cost large-scale production using established complementary metal-oxide semiconductor (CMOS) fabrication infrastructure. Most recently, a mid-infrared comb (1.5 μm to 3.3 μm) has been achieved from a silicon nanophotonic wire with only 16 pJ of coupled pulse energy and its phase coherence was verified by beat note measurements with several narrow line-width sources [35].

Here we present the first f_{CEO} detection of a modelocked laser based on a CMOS-compatible platform using Si_3N_4 waveguides for highly efficient broadband coherent SCG pumped in the 1-μm regime. We show CEO-beat signals from both a 100-MHz DPSSL with a high signal-to-noise ratio of > 25 dB and a 1-GHz DPSSL with > 30 dB. Advances in the growth of thick low-loss Si_3N_4 layers (> 500 nm) of optical quality have enabled the fabrication of dispersion-engineered, low-loss waveguides [33, 34, 36], establishing Si_3N_4 as a promising platform for SCG. Due to its large energy bandgap, Si_3N_4 does not suffer from high nonlinear two-photon absorption (TPA) at 1-μm. The high refractive index contrast between Si_3N_4 (core) and silicon dioxide (SiO_2, cladding) allows for tight optical confinement within a waveguide structure. The nonlinear processes necessary for supercontinuum generation are supported by the high nonlinear index n_2 of Si_3N_4 (10 times higher than silica) [37, 38]. The coupled peak power required for octave-spanning SCG is lowered by more than an order of magnitude as compared to previously reported results based on commercially available PCF [20]. Besides the compactness of such waveguide devices and the reduced peak power requirement, we expect additional benefits from the adjustable waveguide structure to control dispersion and nonlinearity during pulse propagation. All this makes the approach very

#238286 - $15.00 USD Received 17 Apr 2015; revised 21 May 2015; accepted 24 May 2015; published 3 Jun 2015

attractive for future frequency comb sources based on even more compact ultrafast semiconductor lasers in the multi-gigahertz regime [39].

2. Experimental setup

2.1 100-MHz and 1-GHz SESAM modelocked diode-pumped solid-state lasers (DPSSLs)

The performance of the Si_3N_4 waveguides is demonstrated here using two ultrafast SESAM modelocked DPSSLs. The lasers are based on Yb:$CaGdAlO_4$ (Yb:CALGO) laser gain materials pumped with a multi-transverse-mode laser diodes at a wavelength of 980 nm with emission around 1060 nm. A first series of measurements was done using a 100-MHz pulse repetition rate in order to determine the peak power levels required for octave-spanning SCG while staying at moderate average powers. We then successfully continued with a 1-GHz pulse repetition rate, consequently increasing the average power sent into the waveguides by a factor of 10. By comparing the SC generated in both cases and observing the stability over several hours of continuous operation, we rule out any significant thermal or other average-power related degradation of the waveguide devices. The detailed properties of both lasers are listed in Table 1.

Table 1. Properties of the diode-pumped solid-state lasers (DPSSLs) used for SCG in a Si_3N_4 waveguide

Laser	Megahertz DPSSL	Gigahertz DPSSL
Repetition rate	99.1 MHz	1.025 GHz
Gain medium	3-mm long Yb:CALGO	2-mm long Yb:CALGO
Pump	BMU25A-975-01-R03, Oclaro	LIMO 60-F200-DL980-LM, Lissotschenko Mikrooptik GmbH
Pump wavelength	980 nm	980 nm
Laser output power	< 1.2 W	< 1.7 W
Total output coupling rate	1.4%	2%
Pulse durations	65 – 96 fs	> 63 fs (92 fs after isolator)
Center wavelength	1062 nm	1055 nm
SESAM	Single AlAs–embedded InGaAs quantum well + SiO_2 coating	Single AlAs–embedded InGaAs quantum well (uncoated)
saturation fluence	≈5.8 μJ/cm^2	≈11 μJ/cm^2
modulation depth	≈2.8%	≈1.4%

2.2 The Si_3N_4 waveguides for supercontinuum generation (SCG)

Our SCG platform consists of Si_3N_4 waveguides embedded in SiO_2. The Si_3N_4 is first deposited as a film onto an oxide-clad silicon wafer. The waveguide structure is patterned using electron beam lithography and etched with reactive ion etching. A second layer of SiO_2 is then deposited as a top cladding. The waveguide used for the f_{CEO}-detection is 7.5 mm long, with a cross section of 690 × 900 nm, and is spiraled within a 1 mm by 1 mm square that corresponds to the maximum beam lithography tool field. The radius of the bends is kept greater than 100 μm to minimize additional dispersion effects. The waveguide is tapered to facilitate coupling into the fundamental spatial mode and is designed to end 3 μm before the facet of the SiO_2-clad chip. Light is thus first coupled into the lower-index SiO_2 cladding before entering the Si_3N_4 waveguide, which reduces the coupling losses caused by Fresnel reflection [40]. The propagation losses were measured to be 0.7 dB/cm at a wavelength of 1.55 μm. The dispersion profile is engineered to have two "zero group velocity dispersion wavelengths" (ZDWs), thereby providing a 200 nm window of anomalous group velocity dispersion (GVD) around the pump wavelength (see Fig. 1). The effective nonlinearity γ is 3.25 $W^{-1}m^{-1}$ at 1055 nm.

#238286 - $15.00 USD Received 17 Apr 2015; revised 21 May 2015; accepted 24 May 2015; published 3 Jun 2015

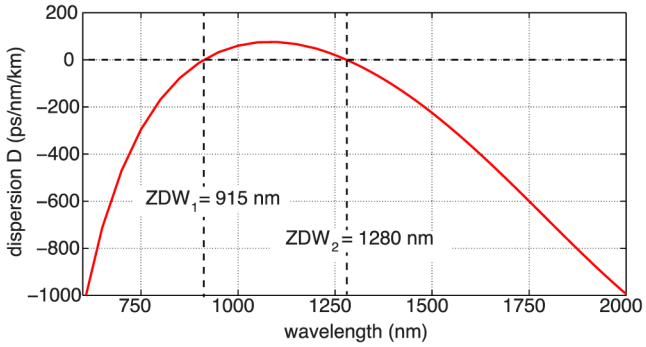

Fig. 1. Simulated dispersion profile of the 690 nm by 900 nm waveguide. The waveguide provides anomalous group velocity dispersion (GVD) around the 1060-nm pump wavelength and has two "zero group velocity dispersion wavelengths" (ZDWs).

2.3 Experimental setup

A complete overview of the experimental setup is shown in Fig. 2. In both laser cavities the output coupler is used in a folding-mirror configuration with two output beams. While one beam was coupled into the waveguide for SCG, the other one was used for further diagnostics.

In case of the 100-MHz laser, we used a dispersion-free variable power attenuation stage consisting of a half-wave plate and a silicon window used in reflection under Brewster angle, enabling tuning of the waveguide input power without altering any other pulse parameters. Before focusing into the waveguide, the size of the collimated beam is adjusted using a telescope and the polarization is rotated with a half-wave plate to match the TE-mode of the waveguide. No optical isolator was needed for the MHz laser, since the back reflections from the waveguide facet did not cause any perturbation.

For the 1-GHz laser the average power incident on the waveguide is a factor of 10 higher to achieve comparable pulse energies. Thus a Faraday isolator was required to block the back reflections from the waveguide. Combined with a half-wave plate, the isolator also acts as a power attenuation stage. The positive group delay dispersion from the isolator is compensated with a transmission grating pair in a double-pass configuration.

In order to detect the CEO frequency of our lasers, the waveguide output is collimated and sent into a quasi-common path *f*-to-2*f* interferometer. The spectral portion around 1360 nm is frequency doubled in a periodically poled lithium niobate (PPLN) crystal and then collinearly recombined in space and time with the 680-nm components of the supercontinuum. After passing through a bandpass filter, the beat signals are detected using a gigahertz avalanche photodiode (APD) and displayed on a microwave spectrum analyzer (MSA).

#238286 - $15.00 USD Received 17 Apr 2015; revised 21 May 2015; accepted 24 May 2015; published 3 Jun 2015

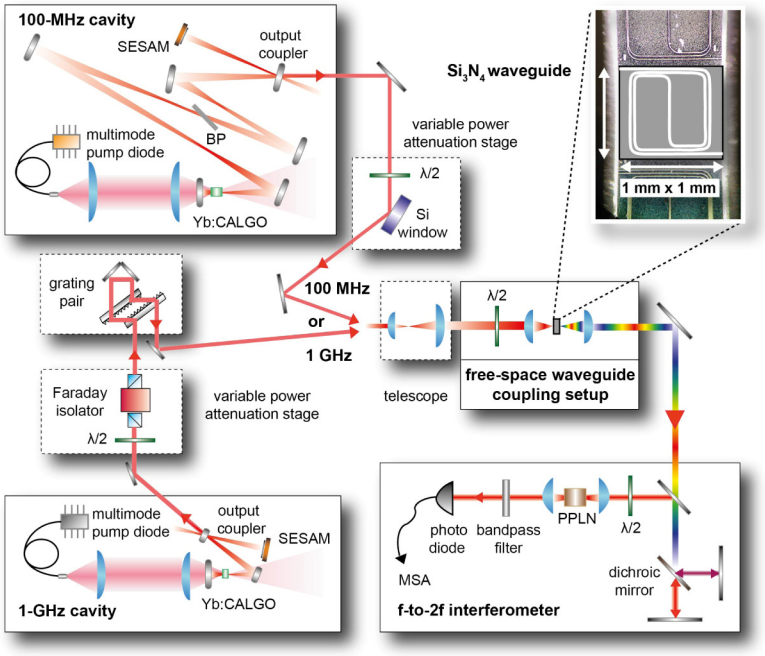

Fig. 2. Overview of the setup: The output of the 100-MHz pulse repetition rate laser (top left) is attenuated to the desired level using a half-wave plate and a Si window under Brewster angle. When using the 1-GHz laser (bottom left), the power is adjusted by rotating the half-wave plate in front of the Faraday isolator. We use a grating pair to compensate for the group delay dispersion in the isolator. After expansion in a telescope and polarization adjustment, the beam is focused into the Si_3N_4 waveguide (top right). The microscope image shows the chip containing several waveguides. The spiraled structure of one waveguide is re-drawn on top for better visibility. The CEO frequency is detected using an *f*-to-2*f* interferometer (bottom right). The dichroic mirror splits the 680-nm and 1360-nm to allow for a variable time delay. Frequency doubling at 1360 nm is then achieved in the PPLN crystal and the SHG signal is collinearly overlapped with the 680-parts of the supercontinuum. After a narrowband optical filter, the beat signals are detected using an avalanche photodiode (APD) and displayed on an microwave spectrum analyzer (MSA).

The f_{CEO}-detection of the 100-MHz laser is performed with 79-fs pulses at a coupled average power of 3 mW (24 mW incident power on the waveguide) and with 92-fs pulses at 37 mW (237 mW incident) for the 1-GHz laser. The characterization of the $sech^2$-shaped input pulses including a second-harmonic intensity autocorrelation, the optical spectrum and a microwave spectrum for both lasers are shown in Fig. 3 and Fig. 4, respectively.

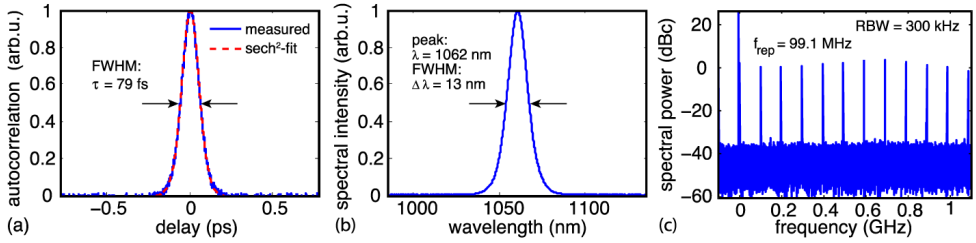

Fig. 3. 100-MHz SESAM modelocked Yb:CALGO laser: (a) Intensity autocorrelation; (b) optical spectrum and (c) microwave spectrum of the 100-MHz laser at a total average output power of 1.05 W. Only 24 mW (3.3 mW coupled) are employed to perform the CEO-beat detection.

#238286 - $15.00 USD Received 17 Apr 2015; revised 21 May 2015; accepted 24 May 2015; published 3 Jun 2015

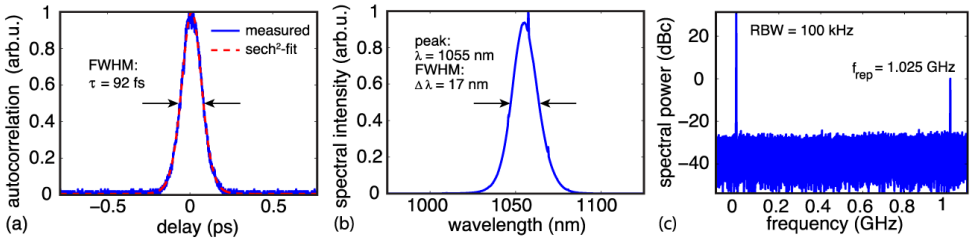

Fig. 4. 1-GHz SESAM modelocked Yb:CALGO laser: (a) Intensity autocorrelation measured after Faraday isolator and gratings; (b) optical spectrum and (c) microwave spectrum of the 1-GHz laser. An average power of 237 mW is sent to the chip (37 mW coupled) to perform the CEO-beat detection.

3. Supercontinuum generation (SCG)

The experimentally observed evolution of the SC with increasing pulse energy is depicted in Fig. 5(a). The coupled pulse energies range from 0.6 pJ to 36 pJ, corresponding to average laser powers from 4 mW to 237 mW of our 1-GHz laser taking into account a coupling efficiency of 15%. The pulses launched into the waveguide at a repetition rate of 1.025 GHz have a duration of 92 fs (after isolator and gratings) and a spectral full-width-half-maximum (FWHM) of 17 nm (see Fig. 4). The supercontinuum extends over almost the full range of the optical spectrum analyzer (OSA) Ando AQ-6315A (specified for 350 – 1750 nm), spanning more than 1.5 octaves (600 nm – 1750 nm)

Figure 5(b) shows the simulated spectra obtained using a split-step Fourier method to solve the generalized nonlinear Schrödinger (GNLS) equation including contributions from third-order nonlinearity, higher-order dispersion, and self-steepening. The dispersion profile (Fig. 1) used for the SC simulations was calculated with a finite element mode solver. The broadening of the SC is in good agreement with the simulations and the spectral parts used for *f*-to-2*f* interferometry are correctly predicted. The best agreement is obtained by re-calibrating the absolute simulated input powers by a multiplication factor of 0.85 compared to the power levels in the experimental case. The slight discrepancy between actual and simulated coupled pulse energies to achieve the same spectral broadening may be due to small amounts of power being coupled to higher-order waveguide modes during propagation.

#238286 - $15.00 USD Received 17 Apr 2015; revised 21 May 2015; accepted 24 May 2015; published 3 Jun 2015

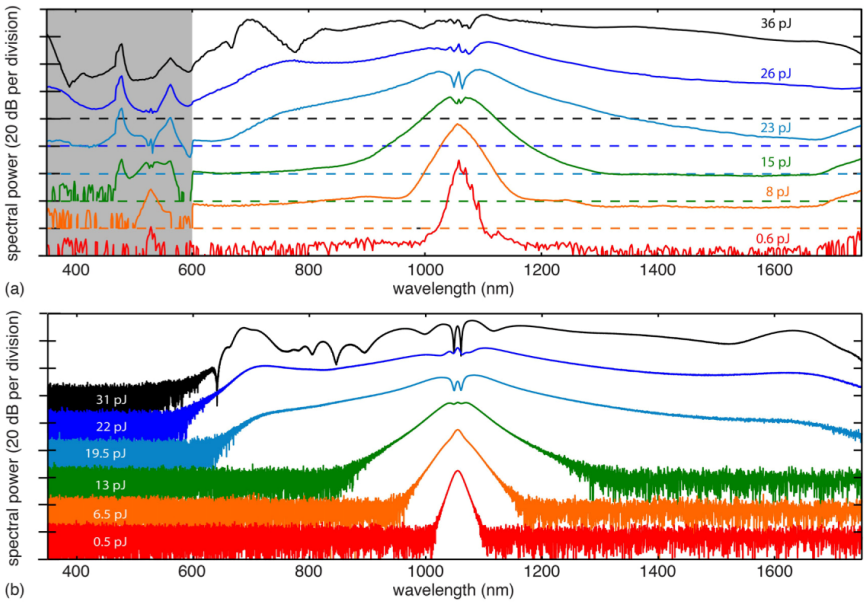

Fig. 5. Supercontinuum (SC): (a) Experimentally observed spectra at different coupled pulse energies, plotted with 20 dB-offsets. The grey shaded area marks the wavelength region where the optical spectrum analyzer (OSA) ANDO AQ-6315A records second-order diffracted light (first-order for > 600 nm) which can generate additional spurious signals not really present in the actual SC. (b) Simulated spectra with the absolute energies re-scaled by a factor of 0.85 compared to the experimental values.

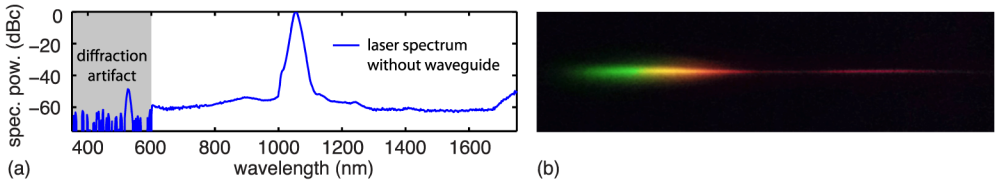

Fig. 6. “Spurious” and “real” frequency components: (a) Spectrum of the gigahertz laser output (Fig. 4b) without spectral broadening in the waveguide recorded with the OSA ANDO AQ-6315A at a RBW of 5nm. Internal filtering imperfections of the OSA can lead to first-order diffracted light of longer wavelengths being recorded again in the short wavelength region (<600 nm), giving rise to a spurious signal peak at half the input wavelength. (b) Photo of the supercontinuum obtained with 36 pJ of coupled pulse energy using a diffraction grating with 1250 lines/mm. Frequency components ranging from green to red are clearly visible by eye, indicating that a “real” spectral content is also present between 500 and 600 nm.

Additionally, we recorded features on our spectrum analyzer in the visible range from 350 nm to 600 nm that are not reproduced by our theoretical model. The OSA Ando AQ-6315A uses second-order diffracted light to detect wavelengths below 600 nm and first-order diffraction for > 600 nm. Spurious signals can thus occur if first-order diffracted long wavelength components are internally not perfectly filtered for the short-wavelength scan (or vice versa). The peak visible already at low pulse energies at exactly half (529 nm) the pump wavelength peak (1058 nm) is such a spurious signal (Fig. 5(a)), further confirmed with the spurious signal shown in Fig. 6(a). We however verified the existence of real spectral components in the 500-600 nm range of the supercontinuum obtained with 36 pJ using the angular dispersion of a simple diffraction grating alone (Fig. 6(b)). Components extending from green to red were clearly visible by eye. Even though the bulk $\chi^{(2)}$ vanishes due to the centrosymmetry of Si_3N_4, a second-order response can arise at the interface of the Si_3N_4 core

#238286 - $15.00 USD Received 17 Apr 2015; revised 21 May 2015; accepted 24 May 2015; published 3 Jun 2015

with the SiO_2 cladding, as demonstrated previously in the case of Si_3N_4 ring resonators [41]. As a consequence, phase matching between the fundamental and higher order waveguide modes can lead to the generation of second or even higher order harmonic components and thus lead to features not predicted by the purely Kerr-effect-based simulations. Coupling to higher order waveguide modes can also lead to slight changes in the effective dispersion profile experienced by the propagating pulse and thus induces a spectral shift of dispersive-wave peaks, which has been shown using algorithms based on pulse propagation in a waveguide with full space- and time-resolution [42]. The higher-order mode effects are not included in our model, as such simulations are several orders of magnitude more computationally expensive compared to solving the GNLS for the fundamental mode, which in most cases already provides very good predictions.

4. Frequency comb offset detection

Using the setup described above, we were able to detect the frequency comb offset, given by the carrier envelope offset (CEO) frequency, of both SESAM-modelocked diode-pumped Yb:CALGO lasers and thus prove that the SC generated in the Si_3N_4 waveguide is highly coherent. In Fig. 7 and 8, we show the detected f_{CEO} beat signals and the corresponding SC spectra that were used for *f*-to-2*f* interferometry. The depicted data was obtained with 30 pJ (36 pJ) of coupled pulse energy, corresponding to 337 W (345 W) of peak power for the 100 MHz (1-GHz) laser.

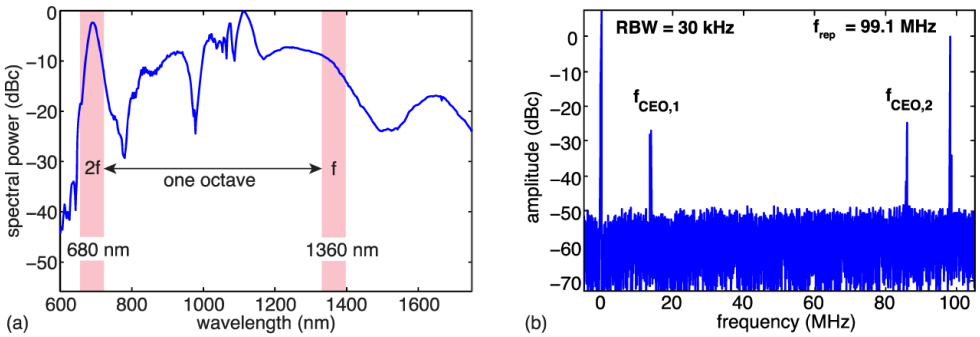

Fig. 7. 100-MHz result: (a) Supercontinuum (SC) obtained with 3.3 mW of coupled average power at 99.1 MHz. The spectral components used for the *f*-to-2*f* interferometry are marked in red. (b) Microwave spectrum showing the pulse repetition rate f_{rep} and the CEO beat frequencies $f_{CEO,1}$ and $f_{CEO,2}$ at 14 MHz and 86 MHz, respectively.

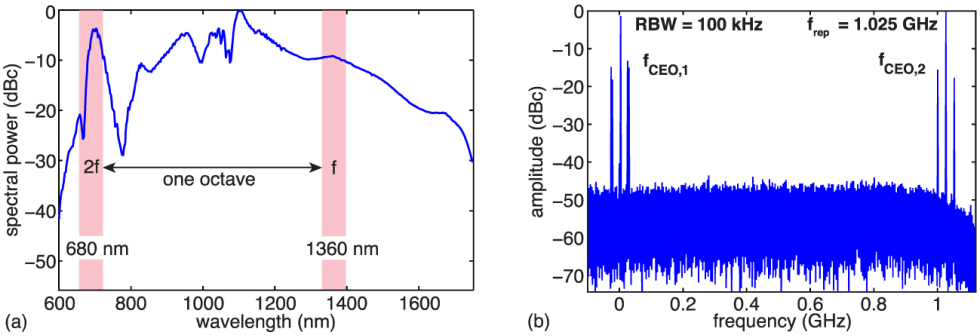

Fig. 8. 1-GHz result: (a) Supercontinuum (SC) obtained with 37 mW of coupled average power at 1.025 GHz. (b) Microwave spectrum showing the pulse repetition rate f_{rep} and the CEO beat frequencies $f_{CEO,1}$ and $f_{CEO,2}$ at 0.024 GHz and 1.001 GHz, respectively.

#238286 - $15.00 USD Received 17 Apr 2015; revised 21 May 2015; accepted 24 May 2015; published 3 Jun 2015

Although the average power was increased by an order of magnitude in the case of the 1 GHz laser to obtain the required peak power, the performance of the waveguide was not affected in any noticeable way, as can be concluded from the similarity of the spectra for 100-MHz and 1-GHz case and the fact that no thermal or material degradation could be observed over several days. A signal-to-noise ratio (SNR) of > 25 dB with a FWHM of ≈0.2 MHz was obtained for the CEO beat of the 100-MHz laser and > 30 dB with a FWHM of ≈2 MHz for the 1-GHz laser. By tuning the laser pump current of the 100-MHz laser to sweep the pulse duration over the whole single-pulse modelocking range from 65 fs (shortest pulses before onset of double-pulsing) to 96 fs (modelocking threshold), we were able to shift the position of CEO beats over a range of 20 MHz, i.e. $f_{rep}/5$. The SNR of the CEO beats is sufficient for additional microwave signal processing, i.e. it will allow us to perform further characterization of the CEO noise properties in the near future. Furthermore, the fact that the CEO beat center frequency can be shifted over a substantial range when adjusting the laser pump power is an essential requirement for ultimately stabilizing the CEO frequency to an external radio-frequency reference by providing feedback to the current of the pump diode.

Table 2. Parameters required for CEO beat detection with a SNR of 30 dB for the same 1-GHz laser using either a 7.5-mm long Si_3N_4 waveguide or 1 m of the commercial PCF NL-3.2-945 from NKT Photonics. Since the PCF is APC-connected, no isolator is required, thus explaining the different pulse durations.

SCG platform	Input	Output	Coupling efficiency	Pulse duration	Coupled peak power	Coupled pulse energy
Si_3N_4 waveguide	237 mW	37 mW	15%	92 fs	0.34 kW	36 pJ
PCF	500 mW	400 mW	80%	63 fs	5.45 kW	390 pJ

In Table 2, we compare the CEO beat detection of our 1-GHz laser using SCG in the Si_3N_4 waveguide to SCG in a 1-m-long commercial PCF (NL-3.2-945, NKT Photonics). Using the same *f*-to-2*f* interferometer as in [20], 16 times less coupled peak power is needed to obtain a comparable SNR (> 25 dB). This important peak power reduction is a consequence of the more than 140 times higher nonlinear coefficient provided in our Si_3N_4 waveguide (3.25 $W^{-1}m^{-1}$) compared to the PCF (0.023 $W^{-1}m^{-1}$). A similar FWHM of the CEO beat (≈2 MHz) is obtained in both cases, indicating that the linewidth of the CEO frequency is not primarily affected by the choice of the supercontinuum platform. The coupling efficiency is defined herein as the ratio of the average power measured free-space directly before and after the waveguide or PCF, respectively. The efficiency of the SCG process in Si_3N_4 can be further increased, as the coupling losses of the waveguides are not fundamental and can be improved by optimization of the taper design and coupling procedure.

5. Conclusion

We have presented the first CEO detection of a modelocked laser based on SCG in a Si_3N_4 waveguide. Strong CEO beat signals (> 25 dB) were obtained for both a 100-MHz and a 1 GHz repetition rate SESAM modelocked diode-pumped Yb:CALGO laser using a standard *f*-to-2*f* interferometer. More than an order of magnitude less coupled peak power is needed to generate an octave-spanning coherent SC from a 1-GHz laser by using a Si_3N_4 waveguide instead of a commercial PCF to achieve a comparable SNR for the same 1-GHz laser.

CMOS-compatibility, compactness and tailored dispersion engineering are convincing assets that Si_3N_4 offers as a platform for self-referencing of modelocked lasers in the 1-μm range. In particular, the low peak power requirement represents an important advantage when going to longer pulses or multi-gigahertz repetition rates and may enable all-semiconductor frequency comb generation directly from compact semiconductor disk lasers such as VECSELs [43, 44] or MIXELs [45] in the near future.

#238286 - $15.00 USD Received 17 Apr 2015; revised 21 May 2015; accepted 24 May 2015; published 3 Jun 2015

Acknowledgments

The authors acknowledge support of the technology and cleanroom facility FIRST of ETH Zurich for advanced micro- and nanotechnology. This work was supported by an ETH grant and the Swiss Innovation Promotion Agency with the CTI contract No. 17137.1 PFMN-NM, and the Air-Force Office of Scientific Research under grant FA9550-12-1-0377. This work was performed in part at the Cornell Nano-Scale Facility, a member of the National Nanotechnology Infrastructure Network, which is supported by the National Science Foundation (NSF) (Grant ECS-0335765). We also acknowledge Ron Synowicki from J.A. Woollam Co., Inc for the characterization of the Si_3N_4 refractive index.

#238286 - $15.00 USD Received 17 Apr 2015; revised 21 May 2015; accepted 24 May 2015; published 3 Jun 2015